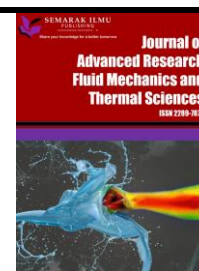




Journal of Advanced Research in Fluid Mechanics and Thermal Sciences

Journal homepage:
https://semarakilmu.com.my/journals/index.php/fluid_mechanics_thermal_sciences/index
ISSN: 2289-7879



Steam Methane Reforming in a Swirling Flow: Effect of Reformer Design Parameters

Igor Karpilov^{1,*}, Ravil Mustafin¹

¹ Department of Industrial Engineering, Faculty of Thermal Engineering, Samara State Technical University, Samara, Russia

ARTICLE INFO

Article history:

Received 15 November 2022

Received in revised form 10 February 2023

Accepted 17 February 2023

Available online 11 March 2023

Keywords:

Steam methane reforming; hydrogen; reformer design

ABSTRACT

Climate change is mostly driven by extensive fossil fuel combustion. Therefore, the transition to clean energy sources and energy efficiency technologies are of great importance. Thermochemical regeneration (TCR) is a method of combined energy efficiency improvement and clean fuel production. Reactor design has a significant impact on the process efficiency and therefore is a key parameter. In the present study, three different reactor geometries were considered: cylinder, square-shaped tube and complicated cylinder. Ansys Fluent was used to model the steam methane reforming reactions in porous media. The influence of the reactor shape on the operating conditions (pressure, velocity, temperature, CH₄ conversion) was assessed. Complicated cylindrical shape produced the highest amount of H₂ but had the highest pressure drop. Square-shaped tube performed better from the production of H₂ per unit of pressure drop perspective. Moreover, the effect of swirled flow on the process performance was studied. In summary, the effective reformer design was chosen and swirl flow suggestions were proposed.

1. Introduction

Modern society is characterized by the growth of energy demand from one hand and requirements for environmental protection from the other. Natural gas is a promising fuel in this perspective due to its superior combustion (high flame temperature) and emission characteristics as it emits lesser CO₂, NO_x and SO₂ particles in comparison to conventional fossil fuels (oil, coal). The main component of natural gas is methane. According to the forecast of the International Energy Agency, the use of natural gas will continue to grow by an average of 2% a year over the next ten years [1].

The main consumer of this fuel is high-temperature installations varying from electricity generation to steel and glass production. These devices need high temperatures for the operation (glass, steel production) as well as for the higher efficiency coefficient (power generation) [2]. In these cases, flue gas temperature can reach 1200°C.

* Corresponding author.

E-mail address: igorkarpilov@mail.ru

<https://doi.org/10.37934/arfmts.104.1.93105>

That exhaust heat could be returned to the cycle as shown in Figure 1 and as a result the unit efficiency will rise [3]. Thermochemical recuperation of initial fuel allows the efficient utilization of the waste heat [4]. That technique is quite modern but very promising [5]. The process essence is in the initial fuel chemical transformation in the course of the highly endothermic reactions [6]. The products of these reactions contain a lot of hydrogen and are usually referred to as syngas. The reactants could vary greatly depending on the operating conditions [7]. In the present paper steam methane reforming reactions are considered as methane is the most widespread fuel.

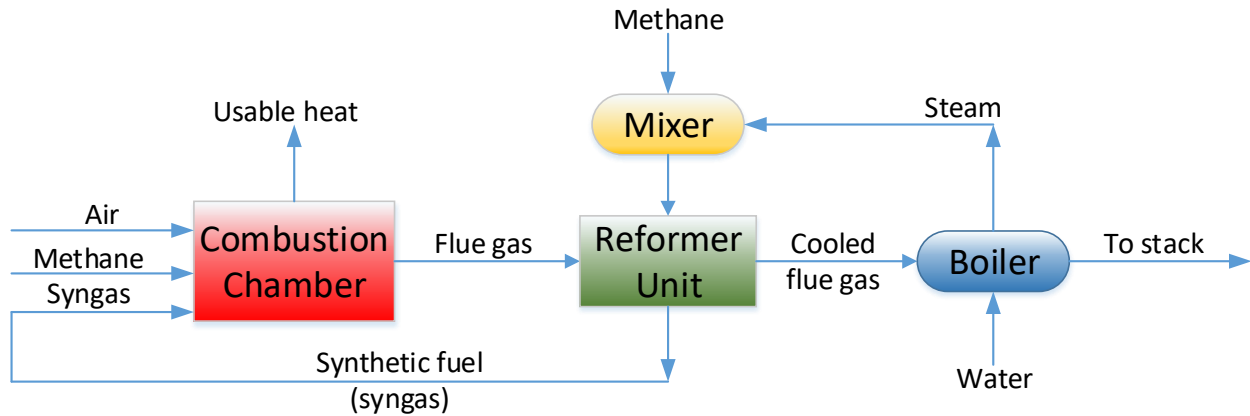


Fig. 1. Principal scheme of thermochemical heat recovery

The latest published articles are focused primarily on steam methane reforming process optimization. The optimal values of temperature, velocity, pressure, steam to methane ratio and oxidizer composition are of great interest. Pashchenko [8] performed the thermochemical analysis of thermochemical waste heat recuperation by steam methane reforming reactions. He determined, that the best recuperation rate was achieved at reformer pressure 5 bar, steam to methane ratio (β) 2:1, at flue gas temperature 900K.

The industrial schemes with the implementation of thermochemical regeneration were assessed by Popov *et al.*, [9]. The authors compared the industrial process scheme in a glass furnace to an upgraded version with thermochemical recuperation and concluded that efficiency could be higher in a range of 10-25% without affecting other parameters of the process.

In the aforementioned articles, the steam methane reforming process was studied by thermochemical analysis in Aspen Hysys and Mathcad. These programs give valuable information on the reaction products but they cannot be used to investigate the distribution of the parameters inside the reactor. A better understanding of this phenomenon is crucial to further reactor performance enhancement. Computer modelling is widely used to evaluate species and temperature distribution, pressure drop and other parameters [10-14].

Articles with steam methane reforming simulations focus on the reforming process optimization. Karthik and Buwa [15] investigated the influence of catalysts with six various shapes on the heat transfer and reaction performance characteristics. He concluded that trilobe-shaped catalysts offer the best trade-off for reaction effectiveness per unit of pressure drop.

Siavashi *et al.*, [16] considered the effect of different porous regions with varying porosities on the steam methane reforming performance. They found that correct porous medium length and porosity enhance the process efficiency up to 116% and 136% accordingly. Also they indicated that optimal flow rate further improves the reaction rate.

The scope of these articles is reformer optimization with different tools. But authors consider only internal packing shape and characteristics. The present study aims at the steam methane

process improvement by assessing three different reformer reactor geometries. The current review was not able to find any existing articles on that topic.

Swirled flow is widespread in combustion processes as it enhances reaction rates by better mixing the reaction products. Therefore, it was decided to study the effect of swirl boundary condition on reaction parameters.

2. Methodology

This study aims to model steam methane reforming reactions and therefore was performed via computer modelling in Ansys Fluent 19 R2 software. Firstly, the computational geometry was created in built-in “Design modeler” CAD software, then the domain was divided into finite-elements via the “Ansys Mesher” tool. Afterwards, the solver settings were specified.

2.1 Model Geometry

Computational geometry comprised of reformer tube and random packing. The considered tube shapes, namely: cylindrical, complicated cylindrical and square are presented in Figure 2. Square shaped reformer tube has a square cross-section while other characteristics are the same. A complicated cylindrical shape differs from the cylindrical one by the narrowing of the cylinder at its center. Therefore, a zone with lesser diameter emerges with a structured packing layer at its center.

The reasons for the study of square-shaped tube originated from aerodynamics study of ventilation shafts. In the square shaped duct, the gas tends to form secondary motions, that influence convective heat transfer and therefore temperature distribution. Complicated cylinder shape was chosen to view the effect of partially structured packing on the reaction kinetics and pressure drop.

In the reformer tube with a diameter of 13mm and length of 320mm 15 cylindrical catalyst particles are randomly placed with a diameter and height of 12mm. The catalyst particles of commercial Ni-based catalyst were used due to their low cost and rather high efficiency. Random packing is the same for all cases so it influences the flow and reaction characteristics similarly. Some space before and after the packing is left for the flow development. The velocity profile before the packed bed forms under the influence of the nearby tube walls. Space after the packing layer is left to stabilize the flow and avoid the backflow effect.

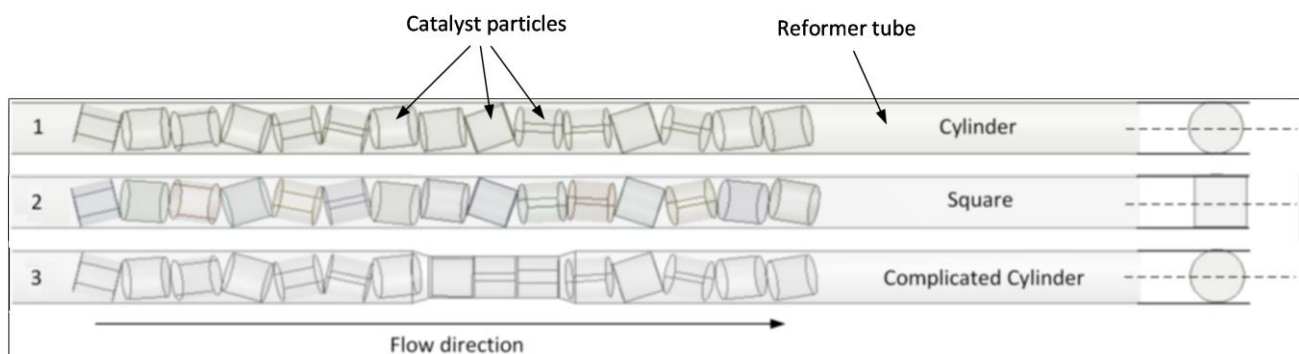


Fig. 2. Computational domains for analyzed reformers: cylinder, complicated cylinder and square

2.2 Mesh

Ansys Fluent solves the model equations by the finite-element approach. The computational domain was divided into tetrahedral elements to obtain the computational mesh. The choice of tetrahedral mesh is motivated by rather complex geometry.

The distance between catalyst wall and tube wall is very small near the contact points. To resolve that issue several techniques are used: bridge contacts, caps and scaling method [17]. Bridges and caps connect the contact points increasing the contact surface whereas scaling method uniformly decrease the catalyst volume and leaves no contact points. In the present study, the catalyst thermal conductivity is rather small and the scaling method is utilized for contact zone treatment.

The computational mesh is shown in Figure 3. It consisted of 5689555 elements for cylinder geometry and varied slightly for other geometries. That rather huge number is a computationally costly decision but it is used to capture the kinetics of the reactions in the thin near-wall region. Moreover, the mesh was additionally refined near the catalyst wall to correctly capture the change in the flow pattern as the mixture flows into the porous region. Empty zones near the inlet and outlet were added to fully develop gas flow and avoid backflow, respectively. The catalyst particles are a porous region that was set according to equations presented in the next section.

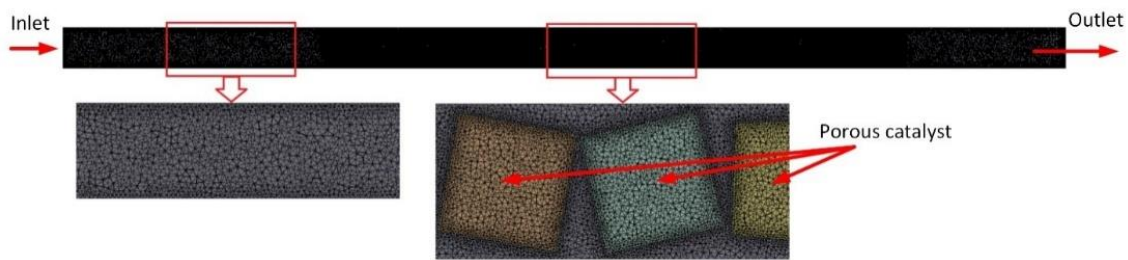


Fig. 3. Computational mesh for cylindrical geometry

2.3 Governing Equation

Modelling presented in this paper accounts for the effects of mass transfer, turbulent effects presented in a narrow channel, heat transfer occurring at the catalyst surface and inside it, flow resistance imposed by the porous media and highly endothermic reactions inside the catalysts.

Equations for mass or continuity conservation are solved in a following form

$$\frac{\partial \rho}{\partial t} + \nabla \cdot (\rho \vec{v}) = 0, \quad (1)$$

where ρ – density, \vec{v} – velocity, t – time.

Eq. (1) is the general form of the mass conservation equation and is valid for both incompressible and compressible flows.

The momentum conservation equation is written

$$\frac{\partial}{\partial t} (\rho \vec{v}) + \nabla \cdot (\rho \vec{v} \vec{v}) = -\nabla p + \nabla \cdot (\vec{\tau}) + \rho \vec{g} + \vec{F}, \quad (2)$$

where $\vec{\tau}$ is the stress tensor, $\rho \vec{g}$ and \vec{F} is gravitational and external force (for example forces emerging due to interaction with dispersed phase), respectively. \vec{F} contains other sources like porous media flow resistance and user-defined sources.

Stress tensor appears as

$$\bar{\tau} = \mu \left[(\nabla \vec{v} + \nabla \vec{v}^T) - \frac{2}{3} \nabla \cdot \vec{v} I \right], \quad (3)$$

where μ – molecular viscosity, I – unit tensor, second term on the right denotes effect due to the volume increment.

To account for the heat transfer phenomena Fluent solves the energy conservation equation

$$\frac{\partial}{\partial t} (\rho E) + \nabla \cdot (\vec{v} (\rho E + p)) = \nabla \cdot \left(k_{eff} \nabla T - \sum_j h_j \vec{J}_j + (\bar{\tau}_{eff} \cdot \vec{v}) \right) + S_h \quad (4)$$

where k_{eff} – effective diffusivity ($k + k_t$, where k_t – turbulent conductivity that changes according to the chosen turbulence model, \vec{J}_j – diffusion flux of species i . First three terms of the right part of Eq. (4) represent energy transfer due to thermal conductivity, particle diffusion and viscous dissipation, respectively.

Turbulence model was chosen k - ω SST according to numerous recommendations stated in the article [18]. That model is widely used to capture effects in the course of chemical reactions. SST differs from the Standard k - ω model by the better wall function that is able to model the flow near the reformer wall in detail without additional inflation layer.

SST model equations describing the turbulence flow are very similar to equations used in the Standard k - ω model and written for k and ω

$$\frac{\partial}{\partial t} (\rho k) + \frac{\partial}{\partial x_i} (\rho k u_i) = \frac{\partial}{\partial x_j} \left(\Gamma_k \frac{\partial k}{\partial x_j} \right) + \tilde{G}_k - Y_k + S_k, \quad (5)$$

$$\frac{\partial}{\partial t} (\rho \omega) + \frac{\partial}{\partial x_i} (\rho \omega u_i) = \frac{\partial}{\partial x_j} \left(\Gamma_\omega \frac{\partial \omega}{\partial x_j} \right) + G_\omega - Y_\omega + D_\omega + S_\omega \quad (6)$$

where \tilde{G}_k – turbulence kinetic generation of turbulence kinetic energy due to mean velocity gradients, G_ω shows generation of ω , Γ_k and Γ_ω represent the effective diffusivity of k and ω , respectively. Y_k and Y_ω describe dissipation of k and ω caused by turbulence, D_ω is a cross-diffusion term. S_k and S_ω are terms specified by user.

The catalyst particles of Ni-Al₂O₃ composition are treated as porous media. Average density is 870 kg/m³ with porosity of 44% (internal porosity) [19]. The media resistance is specified according to the Ergun equations

$$\frac{|\Delta p|}{L} = \frac{150\mu(1-\epsilon)^2}{D_p^2 \epsilon^3} v_\infty + \frac{1.75\rho(1-\epsilon)}{D_p \epsilon^3} v_\infty^2, \quad (7)$$

where $|\Delta p|$ – pressure drop; μ – molecular viscosity; D_p – average particle diameter; L – packing length; ϵ – void fraction of packed bed region (or external porosity) defined as the volume of voids divided by the total packed bed volume.

Porous media is characterized by viscous and inertial resistance coefficients written in form

$$\alpha = \frac{D_p^2 \epsilon^3}{150(1-\epsilon)^2} \quad (8)$$

$$C_2 = \frac{3.5(1-\epsilon)}{D_p \epsilon^3} \quad (9)$$

Steam methane reforming is a set of many chemical reactions occurring simultaneously. The calculation of all reactions takes a lot of computational time and effort and elevates the process accuracy insignificantly. Thus, the scientists proposed simplified approach to the phenomena comprising only 3 main reactions [20]



Reaction rates for reactions (10), (11), (12) are taken as

$$R_1 = \frac{k_1}{p_{H_2}^{2.5}} \left(p_{CH_4} p_{H_2O} - \frac{p_{H_2}^3 p_{CO}}{K_{e1}} \right) \times \frac{1}{Q_r^2} \quad (13)$$

$$R_2 = \frac{k_2}{p_{H_2}} \left(p_{CO} p_{H_2O} - \frac{p_{H_2} p_{CO_2}}{K_{e2}} \right) \times \frac{1}{Q_r^2} \quad (14)$$

$$R_3 = \frac{k_3}{p_{H_2}^{3.5}} \left(p_{CH_4} p_{H_2O}^2 - \frac{p_{H_2}^4 p_{CO_2}}{K_{e3}} \right) \times \frac{1}{Q_r^2} \quad (15)$$

To describe the species rate of formation and dissipation, following equations are utilized

$$r_{CH_4} = R_1 + R_3 \quad (16)$$

$$r_{CO} = R_1 - R_2 \quad (17)$$

$$r_{CO_2} = R_3 + R_2 \quad (18)$$

$$Q_r = 1 + K_{CO} p_{CO} + K_{H_2} p_{H_2} + K_{CH_4} p_{CH_4} + \frac{K_{H_2O} p_{H_2O}}{p_{H_2}} \quad (19)$$

where p_{CH_4} , p_{H_2} , p_{CO} , p_{CO_2} , p_{H_2O} – gas partial pressure, bar; k_r – constant: $k_1 = 9.048 \times 10^{11}$; $k_2 = 5.43 \times 10^5$; $k_3 = 2.14 \times 10^9$. K_{er} – equilibrium constant of reaction r ($r=1,2,3$), K_i – adsorption constant of species i ($i = CO, H_2, CH_4, H_2O$).

2.4 Model Validation

The numerical model should be well-known and confirmed with the experimental data or correspond to the similar data found in the literature. The reformer geometry and considered chemical reactions are similar to the investigated by Karthik and Buwa [15]. Their values are in good agreement with the experimental and numerical findings. Therefore, their results were chosen for validation. The direct comparison was not presented in the current study as in the previous article performed by our scientific group the numerical results were already compared [21]. Values of

velocity, temperature distribution, CH₄ and H₂ mass fractions were in rather good agreement with a maximum deviation of 2.11% for temperature. These results indicate the correct approach for steam methane thermochemical reactions modelling.

2.5 Boundary Conditions

For three different geometries boundary conditions were set the same. At the domain inlet velocity was specified at: 0.3; 0.6; 1.2; 2; 3 m/s, temperature was 1100K and H₂O : CH₄ molar ratio was chosen 2:1, respectively. The solution was performed under atmospheric pressure operating condition. Pressure outlet boundary condition was set at the domain outlet to capture the backflow effects. Adiabatic wall boundary condition was used to treat wall heat flux. Gravitational force was applied in the reformer axial direction.

The steady-state solution was solved until the convergence criteria of 1e-6 for energy and 1e-3 for other variables were met. Second-order discretization was used to calculate the variable values. For pressure-velocity coupling Coupled scheme was utilized.

3. Results

In this section, the results of 3D CFD-modelling are shown, including contours drawn in the reformer central cross-section as well as flow pathlines. Following variables were deemed the most interesting: temperature, H₂ and CH₄ species mass fraction, velocity magnitude and pressure. The other species, namely H₂O, CO and CO₂ are participating in the reaction as well, but H₂O species concentration strongly correlate with CH₄ distribution and CO and CO₂ mass fractions are less significant than H₂ species due to lower calorific value in syngas composition.

3.1 Operating Parameters Comparison

Distributions of temperature for the three geometries considered are depicted in Figure 4. Flow direction is from left to right through the packed bed. Hot water-methane mixture with a temperature of 1100K gradually decreases due to the effect of highly endothermic reactions (10-12). The lowest outlet temperature is observed on the complicated cylindrical geometry, which indicates the most intensive reaction rate. The highest temperature drop is observed in the narrow duct. Cylindrical and square geometry have slightly higher and considerably higher temperature values, respectively. The observed effect is influenced solely by reformer geometry. Therefore, it is an important reformer design feature.

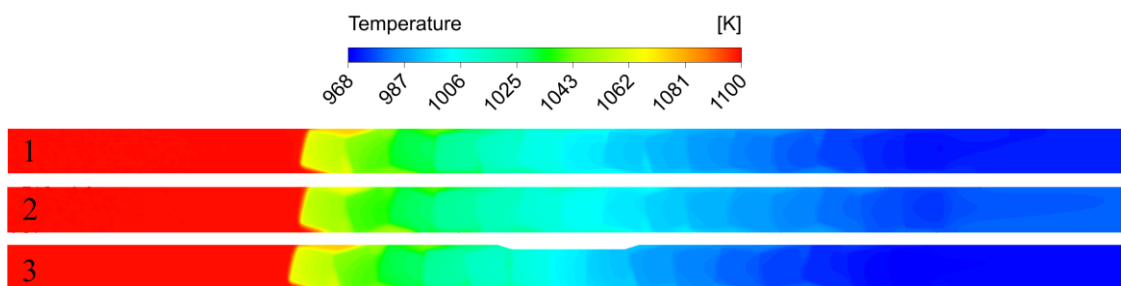


Fig. 4. Temperature contours for cylindrical (1) Square (2) Complicated cylindrical geometry (3) Reactor geometries at inlet velocity 0.3 m/s

To have a better insight into the reaction kinetics contours of the main reactant (CH_4) and product (H_2) were obtained (Figure 5, Figure 6). These species show characteristic reversed concentration: as the reaction progresses CH_4 declines and H_2 increases. The reactions occur only in the catalyst volume and due to the diffusion process species mix homogeneously with the external flow near the wall. The lowest CH_4 and highest H_2 concentrations inside the catalysts are observed on the square geometry. That occurs due to the lower velocity inside the larger square cross-section. Lower velocities inside catalysts on the one hand increase the residence time, on the other, they decrease diffusion process magnitude. As a result, higher H_2 concentration is observed inside the catalyst but a lower average concentration is measured in the whole flow. Complicated cylinder geometry allows better mixing and higher reaction rates in the narrow duct. Therefore, its performance is the best from the H_2 production perspective.

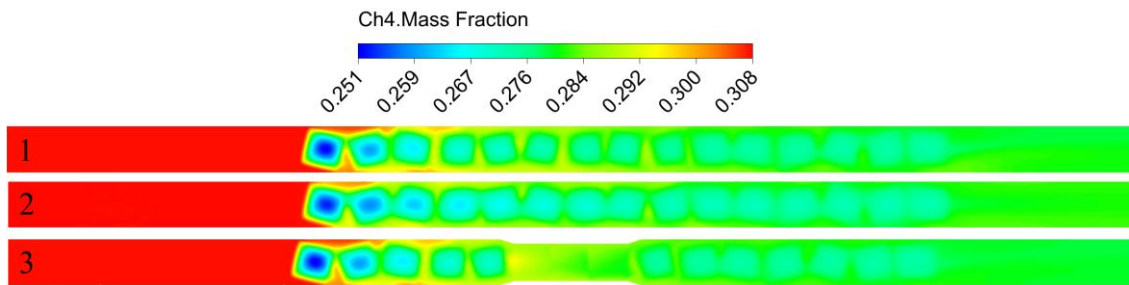


Fig. 5. CH_4 mass fraction distribution for (1) Cylindrical (2) Square (3) Complicated cylindrical geometry at 0.3 m/s

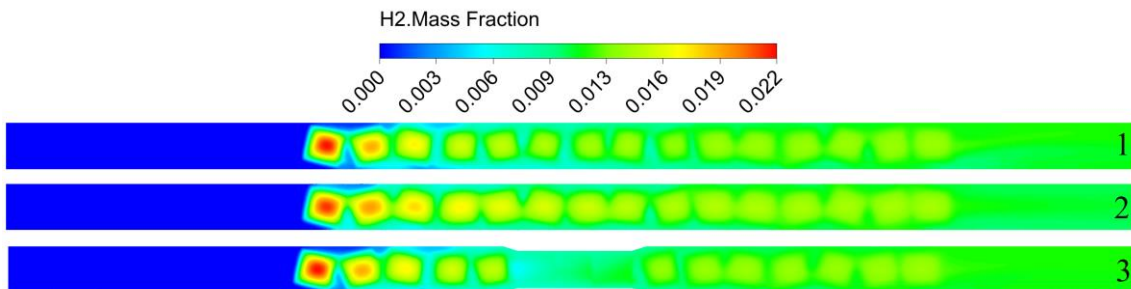


Fig. 6. H_2 mass fraction distribution for (1) Cylindrical (2) Square (3) Complicated cylindrical geometry at 0.3 m/s

Reformer design should not only effectively produce syngas but also have a minimal pressure drop. A large pressure drop causes the efficiency coefficient to drop as power is required to drive the pump. The pressure contours are presented in Figure 7. Absolute pressure steeply decreases from left to right because the high local resistance imposed by the catalyst greatly affects the flow. Cylindrical and square geometries offer relatively small pressure drop of 14 and 3 Pa, respectively, whereas complicated cylindrical reformer offers 140 Pa.

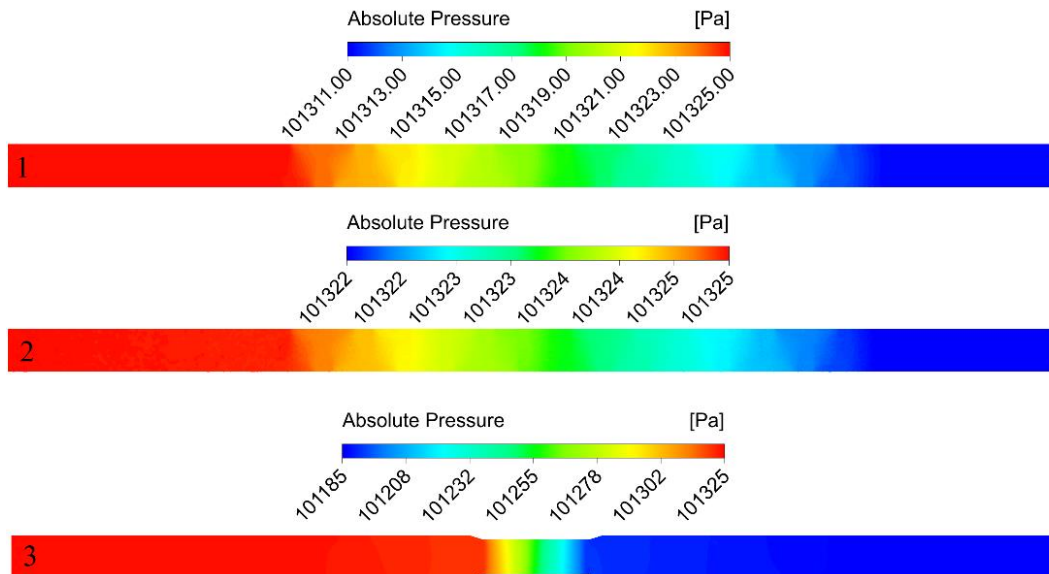


Fig. 7. Absolute pressure values for (1) Cylindrical (2) Square (3) Complicated cylindrical geometry at 0.3 m/s

Velocity distribution sheds the light on the flow pattern, which influences greatly flow residence time and heat transfer properties. In Figure 8 velocity magnitude in reformer central cross-section and on the catalyst surface with volumetric flow pathlines are shown. The square-shaped reformer offers the lowest velocities both inside and outside of catalysts due to the higher cross-section area. The cylindrical shape is characterized by the high velocities in between the reformer wall and catalysts. A complicated cylindrical reformer has the highest velocity magnitude in the whole volume and inside a narrow duct especially. Higher velocity in the narrow duct allows intensified flow contact with the catalyst at a price of high pressure drop [22].

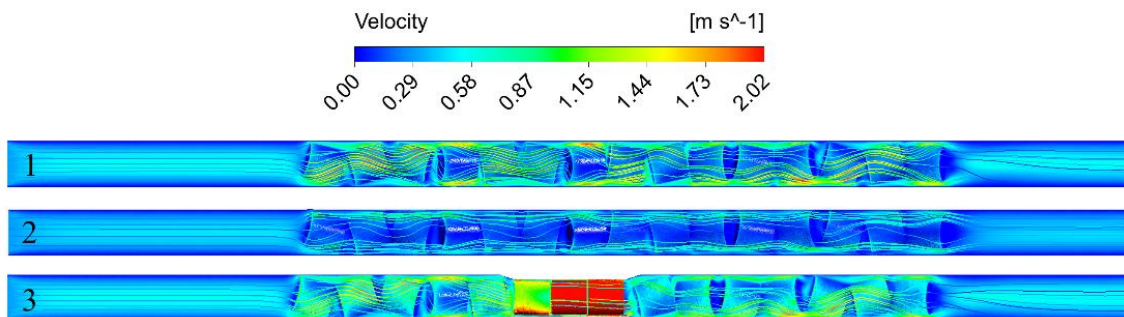


Fig. 8. Velocity contours and volumetric pathlines for (1) Cylindrical (2) Square (3) Complicated cylindrical geometry at 0.3 m/s

The effect of reformer shape at different inlet velocities on H₂ outlet molar fraction and pressure drop is depicted in Figure 9. Pressure drop is rising by a characteristic quadratic dependence while the velocity is elevating. It is notable that at a velocity of 3 m/s pressure drop on the cylindrical and complicated cylindrical shape is by 453% and 3557% higher than on square shape. H₂ molar fraction decreases steadily with the velocity increment due to the lesser residence time. The complicated cylindrical shape offers the highest H₂ yield while cylindrical reformer generates a bit less (by 4%) and square geometry has significantly lesser values (by 20%). As a result, a complicated cylindrical shape is ineffective due to not very high H₂ generation with significant pressure loss. Square shape offers the lowest pressure drop but H₂ outlet concentration is by 16% lower than a cylindrical shape. The

cylindrical shape is good in cases with low inlet velocities where absolute pressure drop is insignificant.

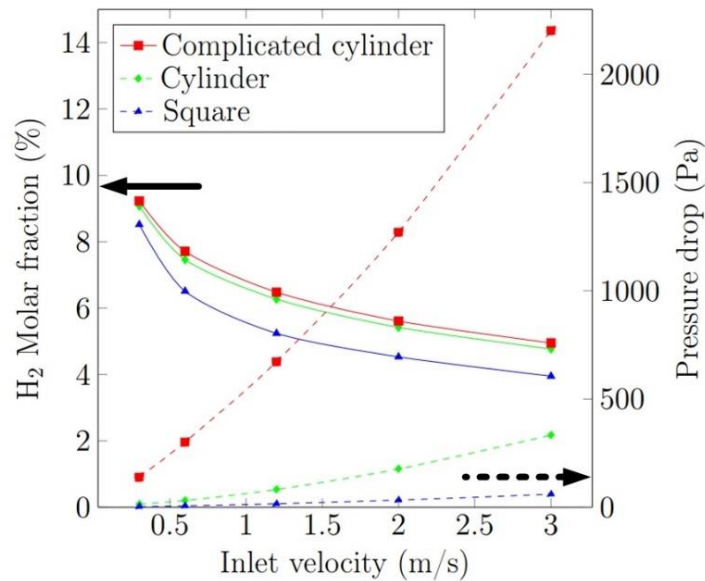


Fig. 9. Comparison of H₂ molar fraction at the reformer outlet and resulting pressure drop

3.2 Swirled Flow Influence

In combustion chambers air swirling is widely used to enhance air and fuel mixing, which allows effective contact and as a result better reaction rate. In thermochemical recuperation reaction occurs mainly inside porous catalyst and on the catalyst surface [23]. Better mixing can allow a higher reaction rate on the catalyst wall and improved CH₄ + H₂O mixture access in zones with very intensive reactions.

These assumptions were enough to test the swirl effect on reaction performance. First experiment was conducted on cylindrical geometry at air inlet 3 m/s. Swirl angle was 45° and tangential velocity 4.5 m/s. In Figure 10 and Figure 11 the simulation results for velocity and temperature are presented. Velocity contour and volumetric pathlines (Figure 10(a)) show a very swirled flow in the beginning (right part) of the tube, which decreases rather rapidly. The flow changes on the first catalyst are observed and practically identical flow is seen further. Temperature contour (Figure 11) indicate no distinct contrast; therefore, reaction kinetics is generally the same.

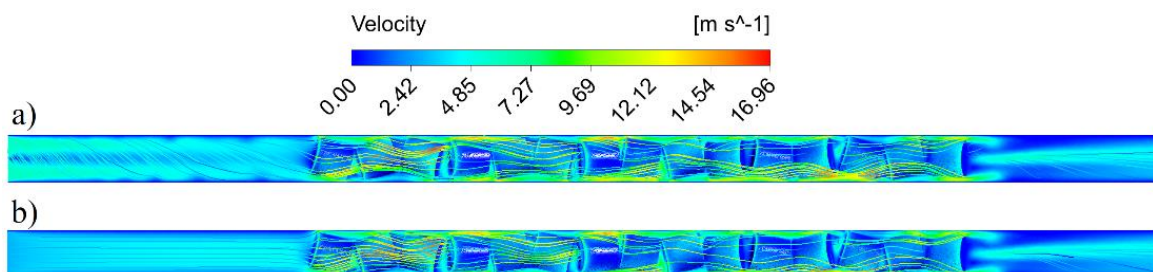


Fig. 10. Velocity contours and volumetric pathlines for (a) Swirled (b) Non-swirled flow at inlet velocity 3 m/s

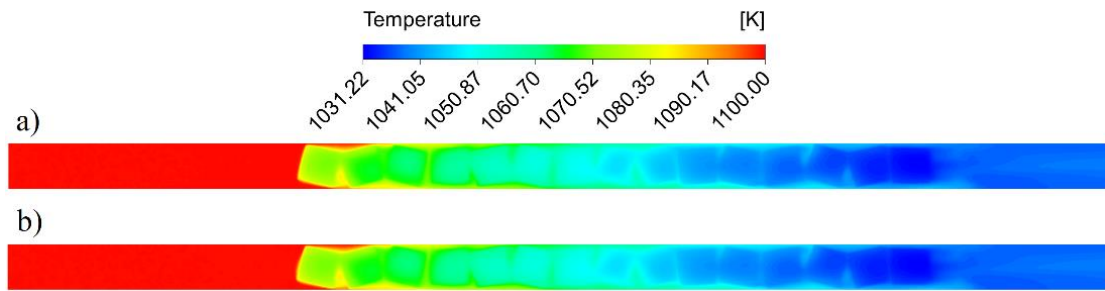


Fig. 11. Temperature contours for (a) Swirled (b) Non-swirled flow at 3 m/s

The swirled-flow effect could be observed better if it is enhanced enough. So the inlet velocity was elevated up to 15 m/s with scaled swirl settings. In Figure 12 and Figure 13 velocity and temperature contours are shown. Swirl became stronger and changed flow on first 2 catalysts, temperature was also lower by 0.5 K. Reaction rate was negligibly enhanced so it can be concluded that swirled flow has practically no effect on reaction performance with current geometry. Model geometry is distinguished by considerable effect from the wall functions. The wall friction influences the swirl dissipation heavily, therefore in tubes with larger diameter the effect from friction will be less pronounced [24]. Presumably, the swirl effect will influence the reaction rate more if the reformer diameter will be higher.

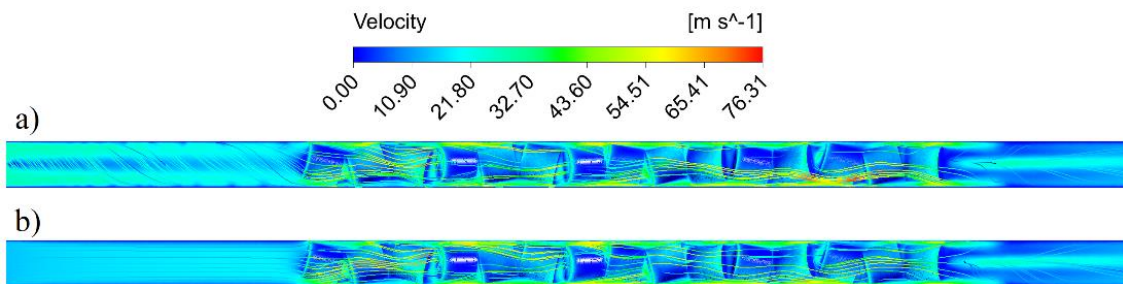


Fig. 12. Velocity contours and volumetric pathlines for (a) Swirled (b) Non-swirled flow at inlet velocity 15 m/s

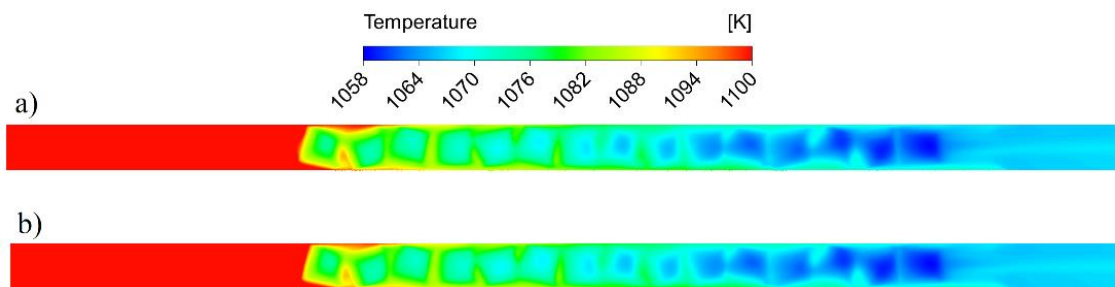


Fig. 13. Temperature contours for (a) Swirled (b) Non-swirled flow at 15 m/s

4. Conclusion

This work aimed to choose optimal reformer geometry for the steam methane reforming process. Three different reformer designs (cylindrical, square and complicated cylindrical tube) were compared through CFD-modelling of reactions in Ansys Fluent 2019 R2 software. Results indicate that complicated cylindrical shape offers the highest H_2 yield while cylindrical reformer generates a bit less (by 4%) and square geometry has significantly lesser values (by 20%). At the same time pressure drop on the cylindrical and complicated cylindrical shape is by 453% and 357% higher than

on square shape. Therefore, square shape is the most effective from the pressure drop per unit mass of generated H₂ perspective. Cylindrical shape is good in cases with low inlet velocities where absolute pressure drop is insignificant.

Swirled flow has practically no effect on reaction performance with current geometry. The swirl effect is considerably diminished by the effect from the wall functions. Presumably, the swirl effect will have a greater influence if the reformer diameter will be higher and packed bed particles will have higher tube-to particle diameter.

Acknowledgement

This work is supported by the Russian Science Foundation under grant 19-19-00327.

References

- [1] Hafezi, Reza, AmirNaser Akhavan, Saeed Pakseresht, and David A. Wood. "Global natural gas demand to 2025: A learning scenario development model." *Energy* 224 (2021): 120167. <https://doi.org/10.1016/j.energy.2021.120167>
- [2] Ol'khovskii, G. G. "The Most Powerful Power-Generating GTUs (a Review)." *Thermal Engineering* 68, no. 6 (2021): 490-495. <https://doi.org/10.1134/S0040601521060069>
- [3] Poran, Arnon, and Leonid Tartakovsky. "Energy efficiency of a direct-injection internal combustion engine with high-pressure methanol steam reforming." *Energy* 88 (2015): 506-514. <https://doi.org/10.1016/j.energy.2015.05.073>
- [4] Verkhivker, Gregoriy, and Vladimir Kravchenko. "The use of chemical recuperation of heat in a power plant." *Energy* 29, no. 3 (2004): 379-388. <https://doi.org/10.1016/j.energy.2003.10.010>
- [5] Pashchenko, Dmitry. "Thermochemical waste-heat recuperation as on-board hydrogen production technology." *International Journal of Hydrogen Energy* 46, no. 57 (2021): 28961-28968. <https://doi.org/10.1016/j.ijhydene.2020.11.108>
- [6] Karthik, G. M., Abhijeet H. Thaker, and Vivek V. Buwa. "Particle-resolved simulations of catalytic fixed bed reactors: Comparison of turbulence models, LES and PIV measurements." *Powder Technology* 361 (2020): 474-489. <https://doi.org/10.1016/j.powtec.2019.05.012>
- [7] Karthik, G. M., and Vivek V. Buwa. "A computational approach for the selection of optimal catalyst shape for solid-catalysed gas-phase reactions." *Reaction Chemistry & Engineering* 5, no. 1 (2020): 163-182. <https://doi.org/10.1039/C9RE00240E>
- [8] Pashchenko, Dmitry. "Energy optimization analysis of a thermochemical exhaust gas recuperation system of a gas turbine unit." *Energy Conversion and Management* 171 (2018): 917-924. <https://doi.org/10.1016/j.enconman.2018.06.057>
- [9] Popov, S. K., I. N. Svistunov, A. B. Garyaev, E. A. Serikov, and E. K. Temyrkanova. "The use of thermochemical recuperation in an industrial plant." *Energy* 127 (2017): 44-51. <https://doi.org/10.1016/j.energy.2017.03.091>
- [10] Alkasasbeh, Hamzeh. "Numerical solution of heat transfer flow of casson hybrid nanofluid over vertical stretching sheet with magnetic field effect." *CFD Letters* 14, no. 3 (2022): 39-52. <https://doi.org/10.37934/cfdl.14.3.3952>
- [11] Al Doori, Wadhah Hussein Abdulrazzaq. "Experiments and Numerical Investigations for Heat Transfer from a Horizontal Plate via Forced Convection Using Pin Fins with Different Hole Numbers." *CFD Letters* 14, no. 9 (2022): 1-14. <https://doi.org/10.37934/cfdl.14.9.114>
- [12] Kamarudin, Saddam, Ishkrizat Taib, Nurul Fitriah Nasir, Zainal Ariff Abidin, Hazimuddin Halif, A. M. T. Arifin, and Mohd Noor Abdullah. "Comparison of Heat Propagation Properties in Different Sizes of Malignant Breast Tumours using Computational Fluid Dynamics." *Journal of Advanced Research in Applied Sciences and Engineering Technology* 28, no. 3 (2022): 368-375. <https://doi.org/10.37934/araset.28.3.368375>
- [13] Jamalabadi, Mohammad Yaghoub Abdollahzadeh. "Parameter study of porosity effects on surface temperature for a porous block under wind, water source and thermal radiation." *Journal of Advanced Research in Applied Sciences and Engineering Technology* 29, no. 1 (2022): 295-315. <https://doi.org/10.37934/araset.29.1.295315>
- [14] Pashchenko, Dmitry. "Industrial furnaces with thermochemical waste-heat recuperation by coal gasification." *Energy* 221 (2021): 119864. <https://doi.org/10.1016/j.energy.2021.119864>
- [15] Karthik, G. M., and Vivek V. Buwa. "Effect of particle shape on fluid flow and heat transfer for methane steam reforming reactions in a packed bed." *AIChE Journal* 63, no. 1 (2017): 366-377. <https://doi.org/10.1002/aic.15542>
- [16] Siavashi, Majid, Farzad Hosseini, and Hamid Reza Talesh Bahrami. "A new design with preheating and layered porous ceramic for hydrogen production through methane steam reforming process." *Energy* 231 (2021): 120952. <https://doi.org/10.1016/j.energy.2021.120952>

- [17] Dixon, Anthony G. "Local transport and reaction rates in a fixed bed reactor tube: Endothermic steam methane reforming." *Chemical Engineering Science* 168 (2017): 156-177. <https://doi.org/10.1016/j.ces.2017.04.039>
- [18] GM, Karthik, and Vivek V. Buwa. "Particle-resolved simulations of methane steam reforming in multilayered packed beds." *AIChE Journal* 64, no. 11 (2018): 4162-4176. <https://doi.org/10.1002/aic.16386>
- [19] Pashchenko, Dmitry. "Pressure drop in the thermochemical recuperators filled with the catalysts of various shapes: a combined experimental and numerical investigation." *Energy* 166 (2019): 462-470. <https://doi.org/10.1016/j.energy.2018.10.084>
- [20] Hoang, D. L., S. H. Chan, and O. L. Ding. "Kinetic and modelling study of methane steam reforming over sulfide nickel catalyst on a gamma alumina support." *Chemical Engineering Journal* 112, no. 1-3 (2005): 1-11. <https://doi.org/10.1016/j.cej.2005.06.004>
- [21] Pashchenko, Dmitry, and Anton Eremin. "Heat flow inside a catalyst particle for steam methane reforming: CFD-modeling and analytical solution." *International Journal of Heat and Mass Transfer* 165 (2021): 120617. <https://doi.org/10.1016/j.ijheatmasstransfer.2020.120617>
- [22] Pashchenko, Dmitry, Igor Karpilov, and Ravil Mustafin. "Numerical calculation with experimental validation of pressure drop in a fixed-bed reactor filled with the porous elements." *AIChE Journal* 66, no. 5 (2020): e16937. <https://doi.org/10.1002/aic.16937>
- [23] Pashchenko, Dmitry. "Hydrogen-rich fuel combustion in a swirling flame: CFD-modeling with experimental verification." *International Journal of Hydrogen Energy* 45, no. 38 (2020): 19996-20003. <https://doi.org/10.1016/j.ijhydene.2020.05.113>
- [24] Liu, Yuyang, Yu Rao, and Bernhard Weigand. "Heat transfer and pressure loss characteristics in a swirl cooling tube with dimples on the tube inner surface." *International Journal of Heat and Mass Transfer* 128 (2019): 54-65. <https://doi.org/10.1016/j.ijheatmasstransfer.2018.08.097>